

Prediction of the Drop Impact Performance of a Glass Reinforced Nylon Oil Pan

Peter H. Foss

*Manufacturing Systems Research Lab
General Motors Global Research and Development
30500 Mound Rd.
Warren, MI 48090*

Abstract

Glass fiber filled plastics are commonly used in automotive applications where increased stiffness and strength are desired. However, widespread application of glass filled thermoplastic materials to automotive components has been limited in many cases by our inability to accurately predict performance and durability. Unfortunately, in complex automotive parts with variable thicknesses, ribs, bosses and other geometric features, both the magnitude and direction of the fiber orientation varies significantly throughout the part. One dominant factor, often ignored during the design phase, is the gate location(s). In addition, processing variables such as melt temperature, mold temperature, fill time, etc. can also affect the fiber orientation to a limited degree. These complex three dimensional fiber orientation patterns result in process-driven position-dependent anisotropic material properties including stiffness, yield and ultimate strength, creep, fatigue, etc.

As part of a cooperative development project between General Motors, BASF and Montaplast, a glass reinforced nylon oil pan was designed, analyzed, molded and tested. The oil pan was molded from BASF's Ultramid[®] B3ZG7 OSI, an "Optimized for Stone Impact" grade of impact modified 35% short glass filled PA6. One of the development tests run on the pans was a drop impact test. In this report we will compare the predicted and experimental impact response using Digimat and LS-DYNA[®] with an anisotropic elastic-viscoplastic material model with failure. The Digimat material model was reverse engineered from high-rate tensile stress-strain data provided by BASF.

INTRODUCTION

In the automotive industry, fiber filled thermoplastics are used in air intake manifolds, radiator tanks, and many other parts. More recently, large quantities of glass filled nylon separator frames have been used in lithium-ion battery packs as part of the thermal management system. Glass filled thermoplastics are also used in virtually every other industry from toys and consumer electronics to business machines and medical devices. Plastic parts have many advantages over metal parts including low mass, design flexibility, and parts consolidation. However, widespread application of glass filled thermoplastic materials has been limited in many cases, especially in automotive applications, by the inability to accurately predict the effect of manufacturing details on part performance and durability.

Fiber filled injection-molded parts contain complex fiber orientation patterns. This fiber orientation state affects material properties including modulus and strength, and part properties including shrinkage and warpage. Tremendous amounts of time and money can be saved if one can predict the moldability and mechanical properties of a part at the design stage.

In the 1990’s, General Motors R&D, General Electric CR&D, HKS (Abaqus) and C-MOLD worked together to develop a framework for structural analysis of parts molded from fiber-filled plastics [1-4]. One major deliverable from the project was the first interface to connect fiber orientation as predicted by a moldfilling simulation with structural analysis via a micromechanics model. In that early work, properties were generally limited to anisotropic linear elastic representations. Fifteen years later, the pioneering work of Doghri, et. al. [5-8] has been implemented in the Digimat software available from e-Xstream engineering [9]. Within the Digimat framework, a material model for a composite is defined by the material properties of the constituents. While the filler materials are generally considered to be linear elastic, the matrix can be defined with varying degrees of complexity, i.e., from a simple linear elastic to a fully thermo-viscoelastic-viscoplastic material. Since the properties of the composite are calculated from the constituents, the composite material will inherit all the features of the isotropic matrix model with the addition of anisotropy due to fiber orientation. Given fiber orientation state predicted by a mold filling simulation (Moldflow, Moldex3D, SigmaSoft, etc.), the Digimat material model will be used to calculate the local anisotropic, strain-rate dependent material response at any point in the structural mesh.

Above the yield stress, the total stress at point can be described as the sum of the yield stress and a hardening stress $R(p)$.

$$\sigma = \sigma_y + R(p)$$

For monotonic loading, p is equal to the plastic strain ϵ_p . Several forms for the hardening stress as a function of plastic strain are commonly used to model the response of real materials, including:

Linear hardening	$R(p) = kp$
Power law hardening	$R(p) = kp^m$
Exponential hardening	$R(p) = R_{\infty} [1 - e^{-mp}]$
Exponential + linear hardening	$R(p) = kp + R_{\infty} [1 - e^{-mp}]$

Where k , kp and R_{∞} are hardening moduli with units of stress and m is the hardening exponent.

In this case, an exponential plus linear hardening model was used since the stress in Figure 1 as a function of strain rate show some slope to the strain-strain curve at failure. However, exponential hardening would give a very similar response.

To capture the strain rate dependence of the composite material, an elastic viscoplastic material model was chosen for the matrix. Since there was minimal effect of strain rate in the elastic region, extension to a fully coupled viscoelastic-viscoplastic model was not warranted. To capture the viscoplastic effects, a hyperbolic sinus law (Prandl law) was chosen to model the plastic strain rate behavior.

$$\dot{p} = \frac{\sigma_y}{\eta} \left(\sinh \frac{f}{\beta} \right)^m$$

The Prandl law was chosen because it has the behavior of shifting the stress-strain response upward at higher strain rates while maintaining similar shape. Other possible functions include the “Current Yield Norton Law” in which the material response becomes more linear at increasing strain rates. Within the range of tested strain rates (0.1 to 100/s), this material does not show this behavior so the Prandl law was deemed more appropriate.

To describe the failure of the composite, the Tsai-Hill 3D Transversely Isotropic Failure criteria was applied in Digimat at the pseudo grain level. In this approach, each material point in the structure is decomposed mathematically into a collection of uniaxial reinforced “grains” at various orientations. The failure of each of those grains was modeled with the Tsai-Hill criteria discussed below. When a user selected fraction of the pseudo grains have failed (0.8), then the material point fails. At that time, the parent finite element simulation will use that flag to control element and node deletion.

The Tsai-Hill 3D Transversely Isotropic Failure criteria has three parameters to describe the experimental failure, X - axial tensile strength, Y - in-plane tensile strength and S - transverse shear strength.

$$f_A = \frac{\sigma_{11}^2}{X^2} - \frac{\sigma_{11}(\sigma_{22} + \sigma_{33})}{X^2} + \frac{\sigma_{22}^2 + \sigma_{33}^2}{Y^2} + \left(\frac{1}{X^2} - \frac{2}{Y^2}\right)\sigma_{22}\sigma_{33} + \frac{\sigma_{12}^2 + \sigma_{13}^2}{S^2} + \left(\frac{4}{Y^2} - \frac{1}{X^2}\right)$$

In practice, the failure parameters are fitted to the experimental data at each strain rate and then interpolated during the finite element simulation to any required local strain rate.

The other important piece of information needed for the reverse engineering was the fiber orientation state of the tested plaques. As shown in Figure 2, this material shows a classic shell-core structure with shell orientations between 0.7 and 0.9. The material shows a relatively broad core with a highly transverse alignment of about 0.05 in the center. The fiber orientation data was measured using the method of ellipses on polished cross sections by Prof. Don Baird's group at Virginia Tech.

REVERSE ENGINEERING

The first step in reverse engineering the material model was determining the matrix elastic modulus and fiber aspect ratio based on the 0 and 90 degree elastic modulus at the lowest (0.1/s) strain rate. Step two was to roughly fit the plasticity parameters to the low strain rate data. Finally all the experimental data was loaded in Digimat-MX and the viscoplastic parameters were fit using MX's optimization system. The results of this global optimization are shown in Figure 3. The experimental curves are shown in dashed format while the reverse engineered model predictions are shown as solid lines. Note the model predictions were calculated out to the final strain point in the experimental data. No failure criteria were used up until this point.

As discussed above, the Tsai-Hill failure parameters were fitted at each strain rate and interpolated for intermediate strain rates during the LS-DYNA simulation of the impact event. In Figure 4, the results of the fitting are shown for the 10/s data. Note in this case, the end points of the 0 and 90 degree data were fitted exactly using the axial and in-plane strength parameters. The shear parameter was selected to give a reasonable response for the shear12 curve. In the absence of experimental data at a third angle (45 degrees), fitting of this parameter was not determinate. As discussed above, this procedure was repeated for the three sets of strain rate data. Because this material model was used in an explicit analysis with LS-DYNA, Digimat's "hybrid" solution method was selected. In this analysis, rather than calculating local mechanical properties for each integration point in the simulation in real time (micro method), the hybrid functionality pre-calculated the stress-strain behavior as a function of fiber orientation and strain rate. During the LS-DYNA simulation, these pre calculated curves are interpolated to describe the local response.

RESULTS AND DISCUSSION

As discussed above, the purpose of this work was to predict the impact response of a glass filled nylon oil pan. The pan was center gated with a single hot runner as shown in Figure 5. Moldflow was used with a 3D mesh to predict the injection molding process and the resulting fiber orientation. The fiber orientations were mapped to the LS-DYNA 3D solid model for the impact simulations as shown in Figure 6. The simulations and experiment used a 25 mm diameter impact probe dropped from 0.762 meters. The drop mass was 22.7 kg and the incoming velocity was 3.7 m/s. With an incident energy of over 150 J, complete failure of the pan was guaranteed. Parallel tests with a 1" steel ball shot at pans with increasing velocity and energy will be reported at a later date.

The experiments and simulations were run in two ways: pan only and full assembly. For the pan only case only the oil pan was tested. In the full assembly case, the system included the pan, pickup tube, windage tray and the external aluminum pan brace. As shown in Figure 7, the assembly, while somewhat stiffer than the pan only, absorbed less energy since it failed sooner than the bare pan.

As shown in Figure 8, both the experiment and the simulations show qualitatively similar failure. As the indenter penetrated the pan, 2-3 cm long pieces of the pan broke free. Note the experimental failure shows cracks propagated parallel to the flow away from the gate. In the simulation, the cracks propagated more radially from the impact point.

As shown in Figure 9, the load-time response was very well predicted by the simulations for both the pan only and assembly cases. The simulation clearly shows the stiffening effect of the assembly over the bare pan. One

significant difference between the simulations and experiment occurs at about 3 ms elapsed time. The load drops fairly significantly due to compressive failure and element deletion on the impact side. Because Digimat coupled with LS-DYNA cannot treat compressive and tensile failures differently, elements that fail in compression are deleted. In reality in most cases that failed material, if failed in compression, would not be “deleted” and would remain between the indenter and impact site. This would prevent the load drops observed in the simulations. Test simulations with the failure criteria turned off did not show these early load drops.

Clearly the simulations show a more gradual failure than observed in the experiments at 4 ms for the pan only and 6 ms for the assembly. The peak time and force agree very well for the assembly runs. The agreement for the pan only was not as good with significant under prediction of the peak load but with good agreement on the failure time (displacement).

As shown in Figure 10, the energy absorbed from the indenter was very well predicted up to the point of failure at 4 ms. The black curve is the experimental energy reported from the Dynatup impact test. This energy was calculated from the incident velocity of the indenter and the force-time response given the mass of the indenter. A similar calculation for the simulation is shown in the red curve in Figure 10. In this case, the current kinetic energy of the indenter was subtracted from its initial energy to create the curve. The agreement was virtually perfect up until the point of failure. However, if one adds up the kinetic, internal and contact energies reported for the entire system except the indenter, the response shown in green was predicted. At the point of failure, 7-8 J of energy have disappeared from the system. Discussions between e-Xstream and LS-DYNA continue to resolve this issue since generally a gain or loss of more than 1% in the total system energy is considered the upper limit for a good simulation.

FUTURE WORK

At this time, simulations of ballistic impact on the pan with a 25 mm steel ball as a function of velocity are underway. Experimental testing has been completed and showed failure energy was similar to the drop tower tests.

Future pan only experiments are planned to provide more accurate results for the pan only and assembly cases. With only the single pan only run, the significance of the difference between the pan only and assembly tests (and simulations) is unknown and would serve as a very good validation of the predictability of the results.

Finally, as e-Xstream develops Digimat, one needs to revisit the failure criteria calibration from the tensile data. In addition to needing 45 degree test data, the failure criteria was fit using a single layer microstructure with the through thickness averaged orientation shown by the dotted line in Figure 2. Investigations using the actual layered microstructure may result in different failure criteria parameters since the shell and core layers may fail at different strains depending on test direction.

ACKNOWLEDGEMENTS

The author would like to thank Kurt Danielson for fitting the EVP material model as well as Bernard Alsteens and Thierry Malo from e-Xstream engineering for many helpful discussions and software support. BASF was an integral partner on this simulation work including building the LS-DYNA and Moldflow models, providing the high strain rate tensile data and performing the drop tower testing.

REFERENCES

1. P. H. Foss, "Coupling Of Flow Simulation And Structural Analysis For Glass Filled Thermoplastics", *Polymer Composites*, 25, 343-354 (2004).
2. B. E. VerWeyst, C. L. Tucker III, and P. H. Foss, *Int. Poly. Proc. Journal*, 12, 238 (1997).
3. C.L. Tucker III and E. Liang, "Stiffness Predictions for Unidirectional short-fiber composites: Review and Evaluation", *Comp. Sci. Tech.*, 59, 655-671(1999).
4. M. Gupta, K. K. Wang, "Fiber Orientation And Mechanical Properties Of Short-Fiber-Reinforced Injection-Molded Composites: Simulated And Experimental Results", *Polymer Composites*, 14, 367-382(1993).
5. I. Doghri and A. Ouair, "Homogenization of Two-phase Elasto-plastic Composite Materials and Structures: Study of Tangent Operators, Cyclic Plasticity and Numerical Algorithms", *Int. J. of Solids and Struct.*, 40, 1681-1712(2003).
6. O. Pierard, C. Friebel and I. Doghri, "Mean-field Homogenization of Multi-phase Thermo-elastic Composites: A General Framework and It's Validation", *Composites Science and Technology*, 64, 1587-1603(2004).
7. I. Doghri and C. Friebel, "Effective Elasto-plastic properties of Inclusion-reinforced Composites: Study of Shape, Orientation and Cyclic Response", *Mechanics of Materials*, 37, 45-68(2005).
8. O. Pierard, J. LLorca, J. Segurado, and I. Dogrhi, "Micromechanics of Particle-reinforced Elasto-viscoplastic Composites: Finite Element Simulations Versus Affine Homogenization", *Int. J Plasticity*, 23, 1041-1060(2007).
9. "DIGIMAT A software for the linear and nonlinear multi-scale modeling of heterogeneous materials." e-Xstream engineering, Louvain-la-Neuve, Belgium.

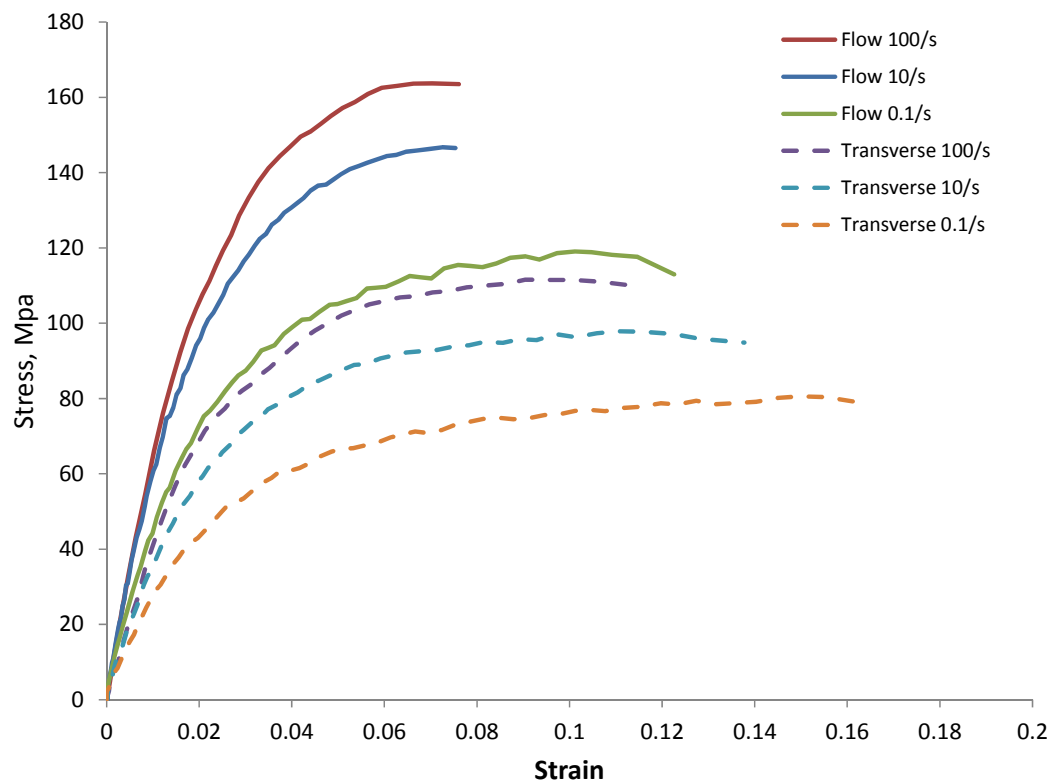


Figure 1. True stress strain response of BASF OSI as a function of strain rate and direction.

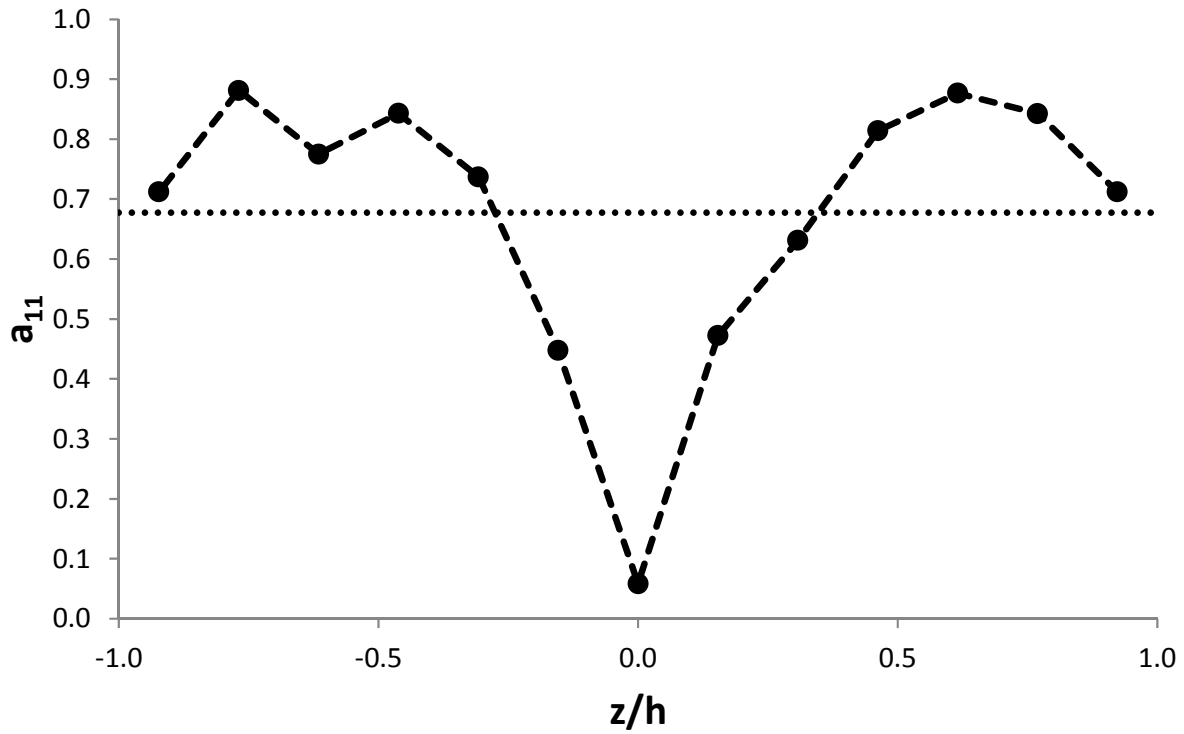


Figure 2. Measured fiber orientation at the center of the plaque used for mechanical property measurements.

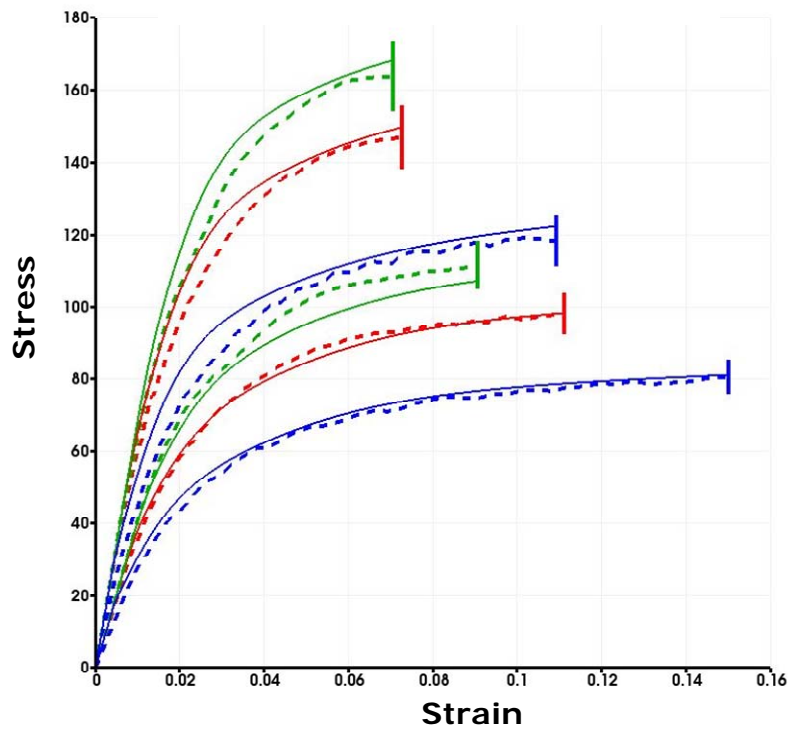


Figure 3. Stress strain response of the reverse engineered elastic-viscoplastic material model (solid lines) and the experimental data (dashed lines) without failure.

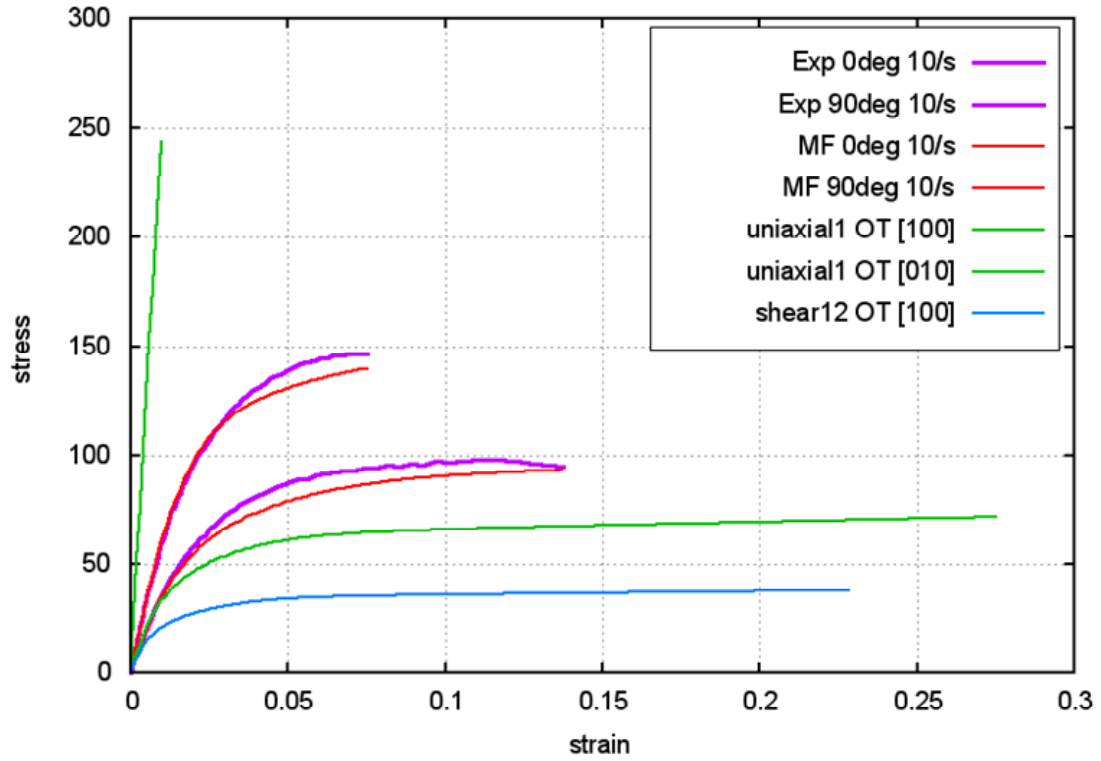


Figure 4. Predicted stress-strain response to failure for an elastic-plastic material. Also plotted are the predictions for a perfectly oriented ($a_{11}=1$) tested at 0 and 90 degrees as well as pure shear.

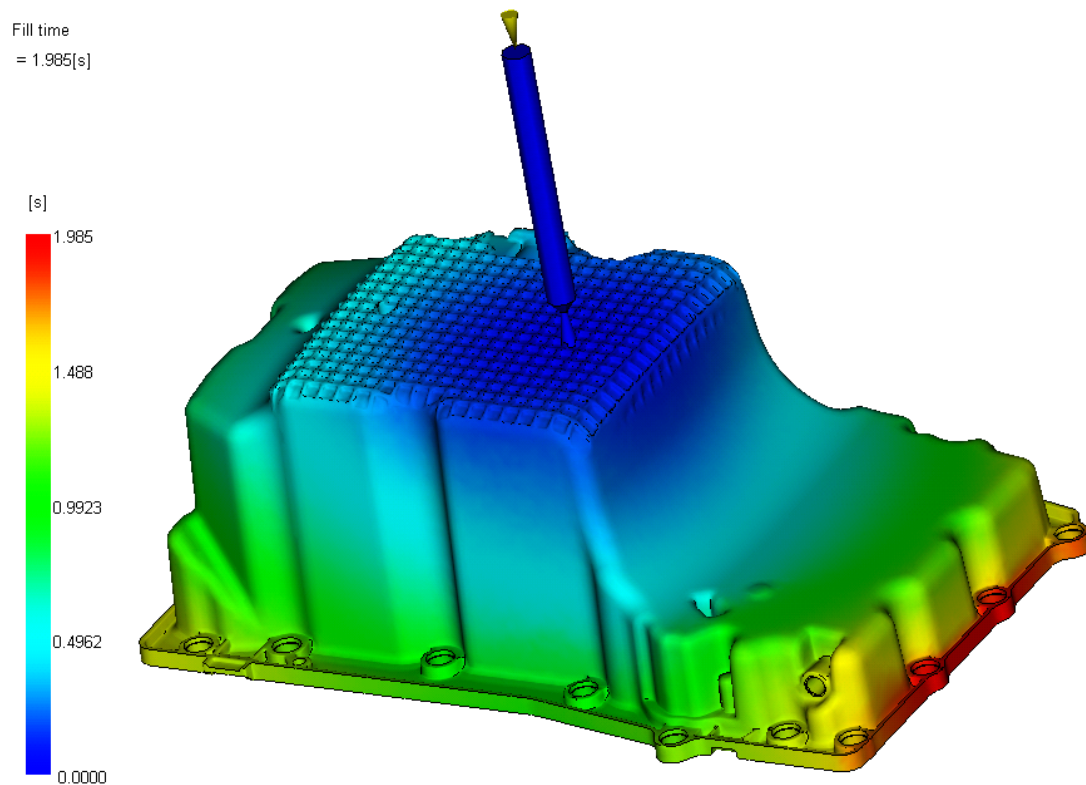


Figure 5. Predicted fill pattern for the injection molded oil pan.

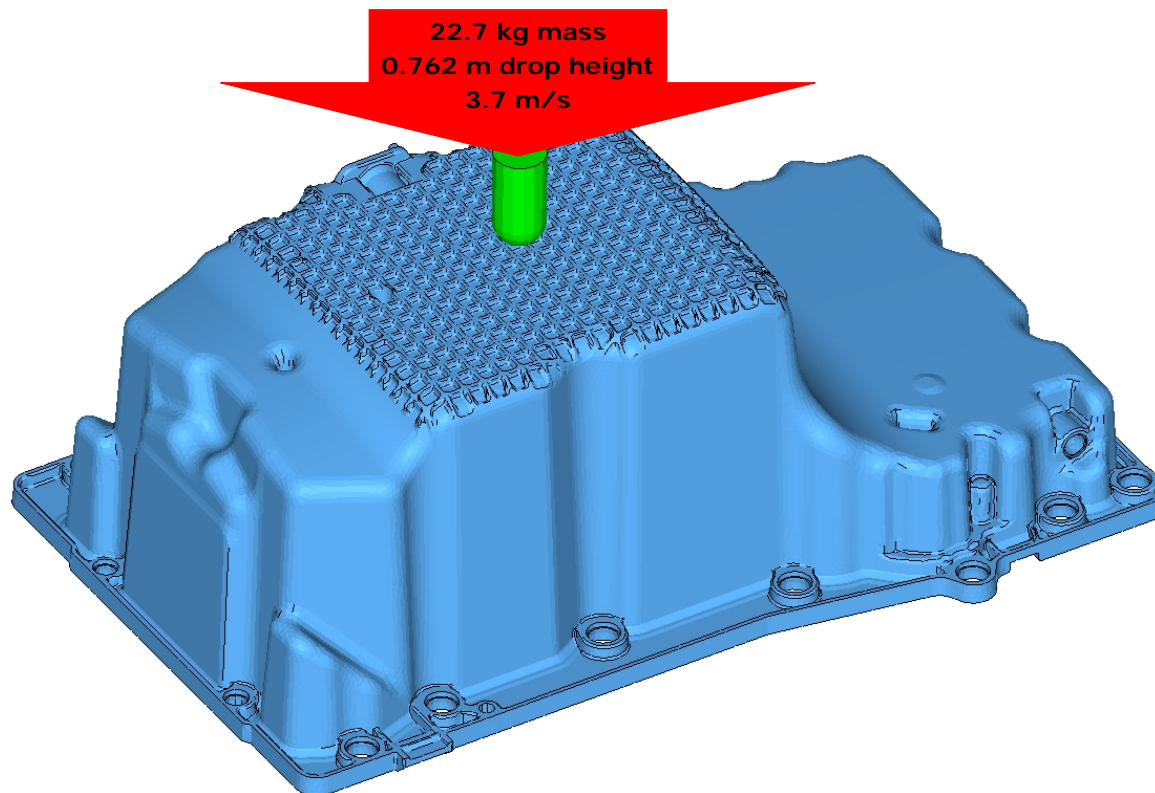


Figure 6. Drop impact setup.

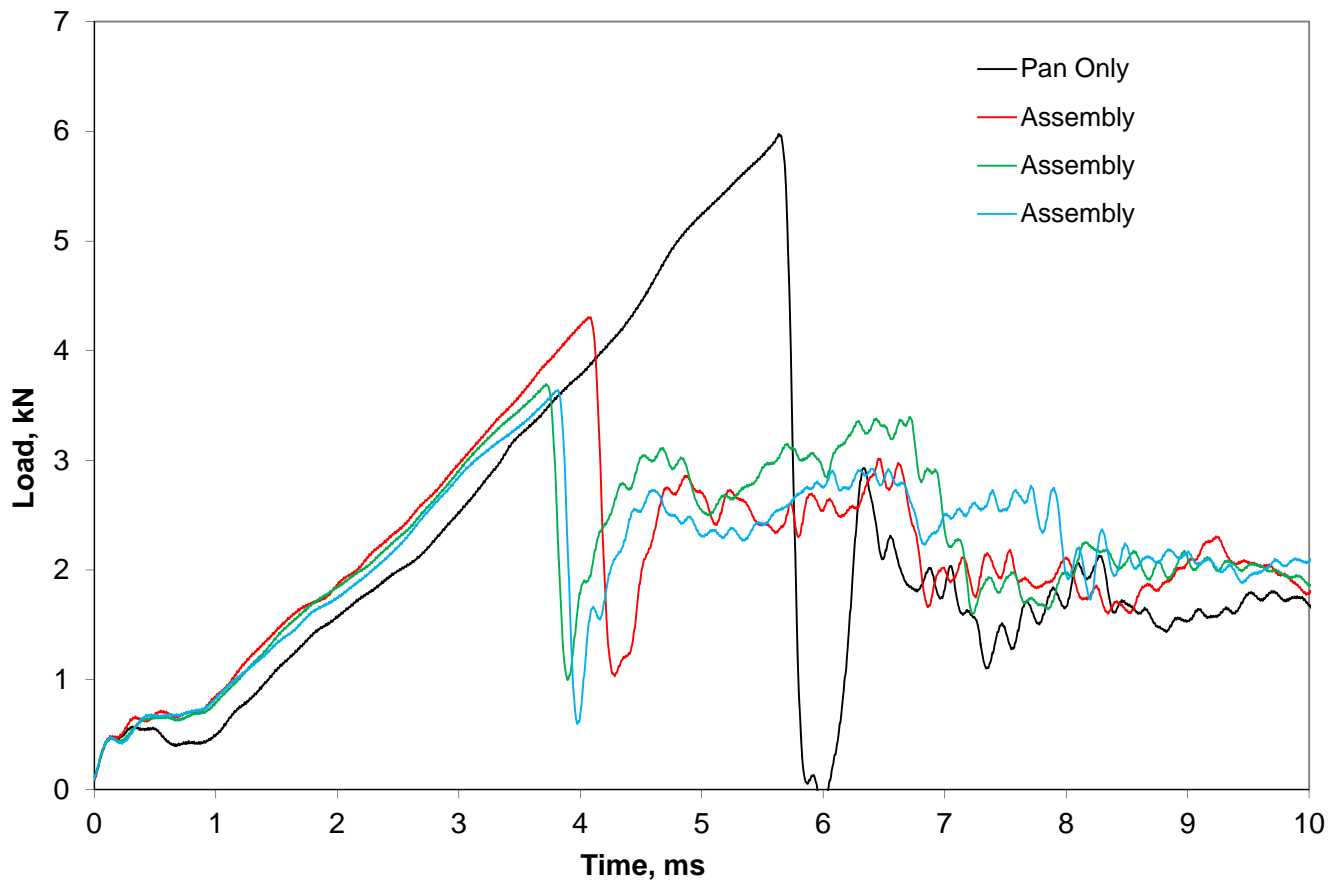


Figure 7. Experimental load-time response of an oil pan only and three full assemblies.

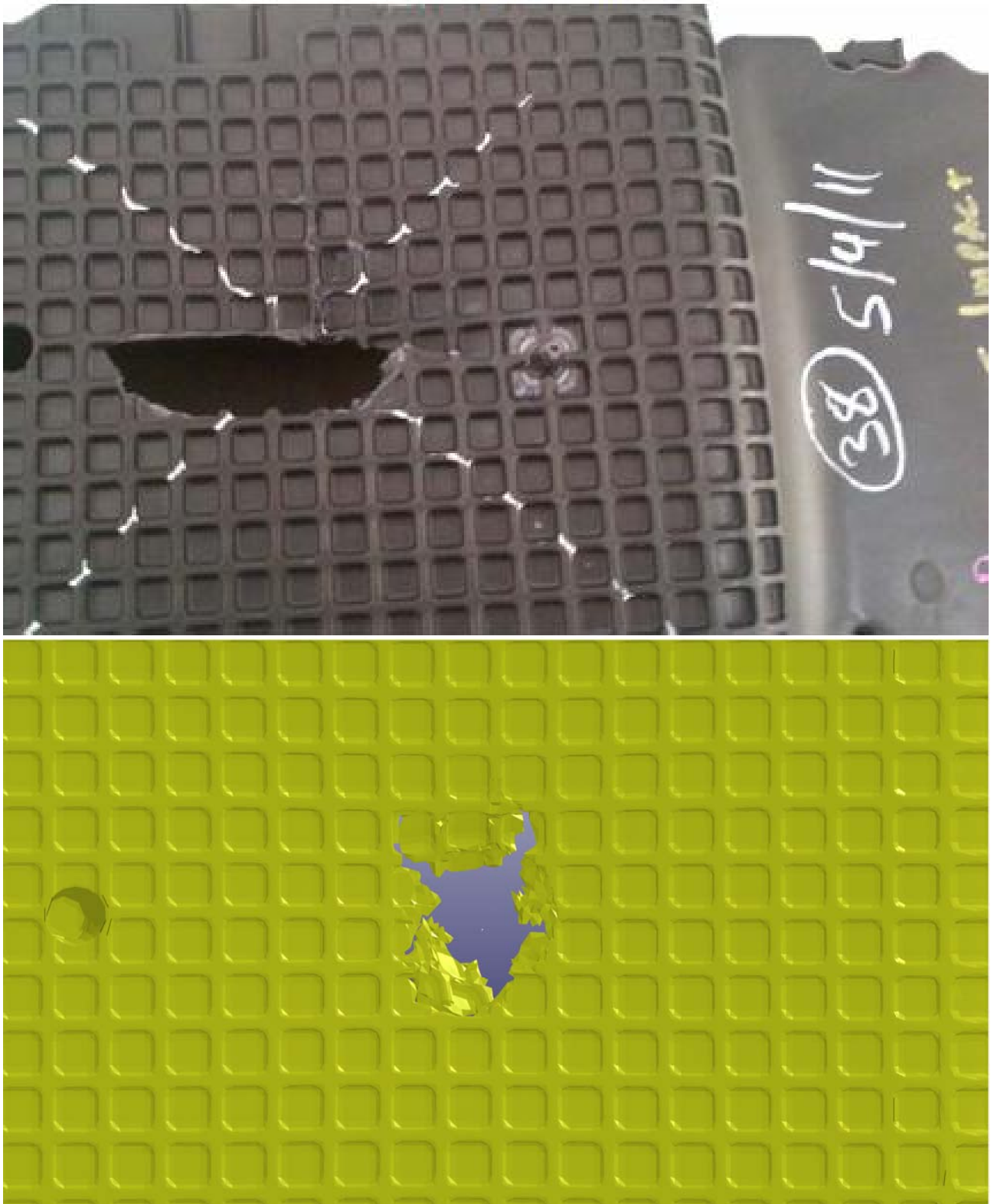


Figure 8. Experimental and predicted failure pattern of the oil pan.

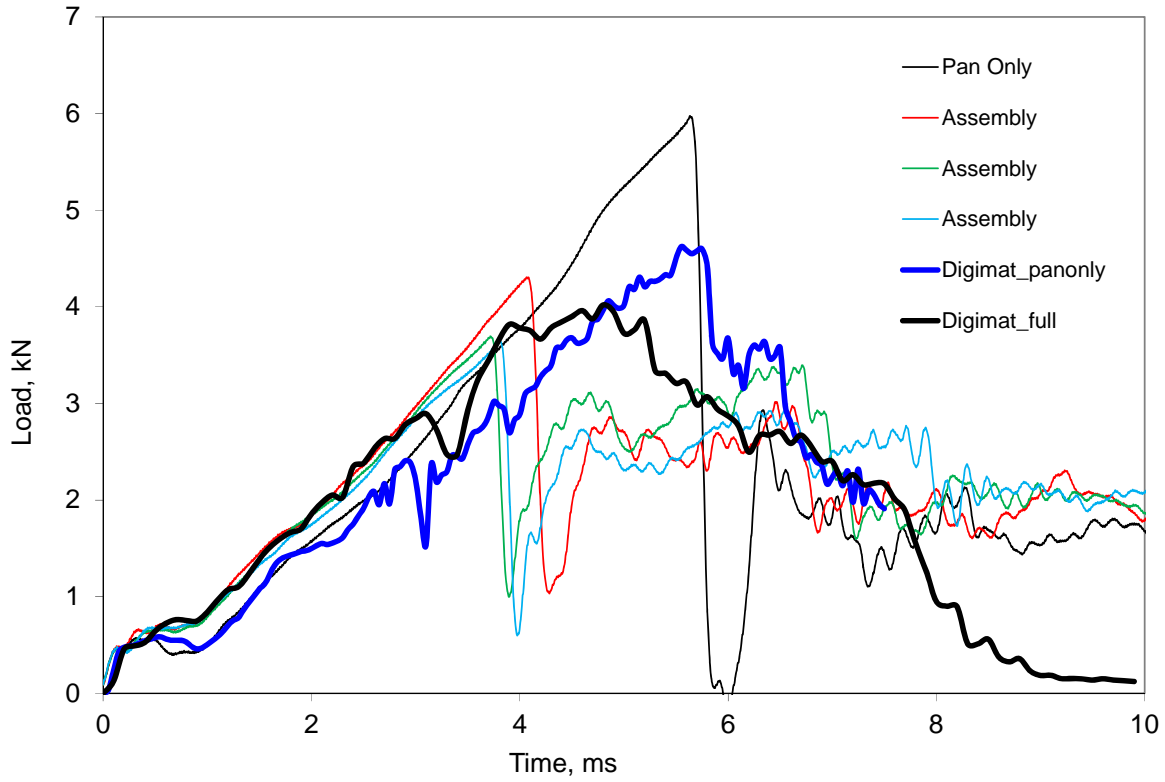


Figure 9. Predicted and experimental load-time response of the oil pan only and the full assembly.

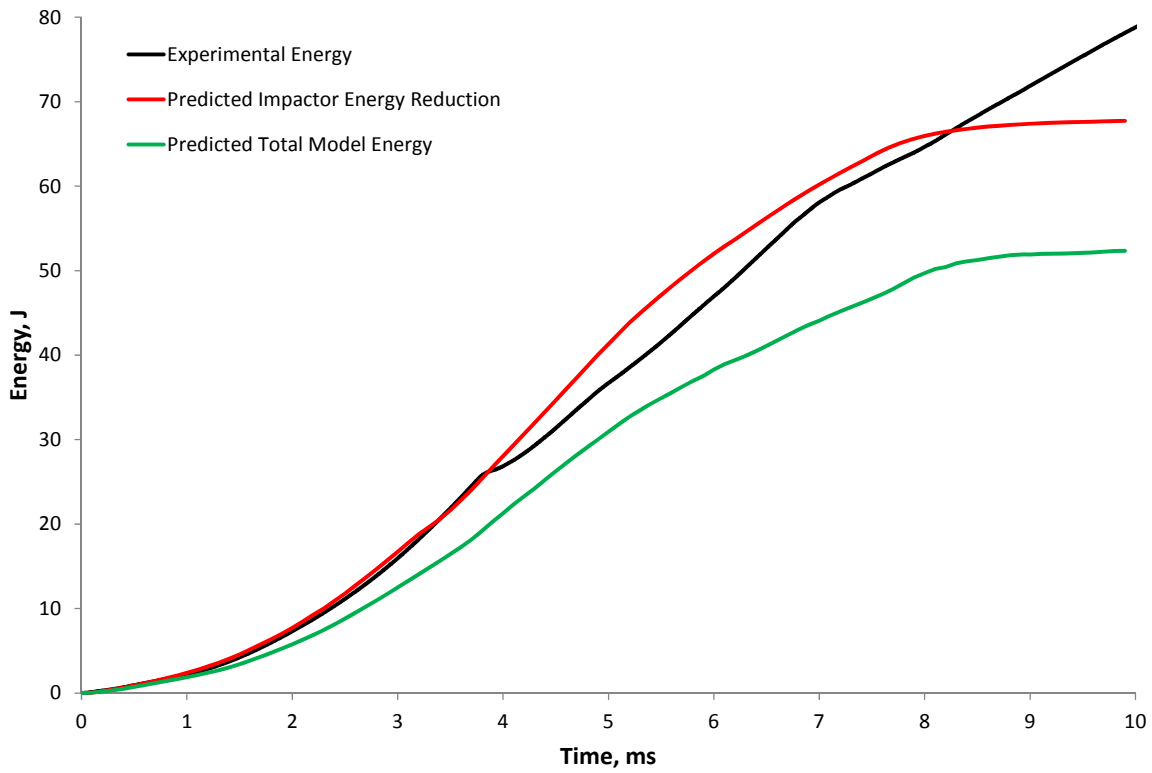


Figure 10. Predicted and experimental energy response of the full assembly.